Hindawi
International Journal of Antennas and Propagation
Volume 2021, Article ID 5439822, 9 pages
https://doi.org/10.1155/2021/5439822

Research Article

Fast Synthesis Method for Large Aperture Array Pattern in the Presence of Array Errors

Lihuan Huo[1,2] **Rulong Bai**[1,2] **Fei Xue**[1,2] **Jianfeng Chen**[1,2] **Penghui Huang**[3] **and Guisheng Liao**[4]

[1]*The 54th Research Institute of CETC, Shijiazhuang 050081, China*
[2]*Hebei Key Laboratory of Electromagnetic Spectrum Cognition and Control (ESCC), Shijiazhuang 050081, China*
[3]*School of Electronic Information and Electrical Engineering, Shanghai Jiao Tong University, Shanghai 200240, China*
[4]*National Laboratory of Radar Signal Processing, Xidian University, Xi'an 710071, China*

Correspondence should be addressed to Lihuan Huo; huolihuan@163.com

Received 4 May 2021; Revised 8 June 2021; Accepted 14 June 2021; Published 30 June 2021

Academic Editor: Mohammad Alibakhshikenari

In this paper, an improved array synthesis method with array errors is proposed for large aperture arrays. Because of the array errors such as amplitude-phase errors and positions errors, the performance of the array synthesis is reduced seriously. Firstly, the ideal fast low sidelobe synthesis method is obtained based on the discrete Fourier transform (DFT) method. Then, by using Taylor expansion to remove the coupling relationship between the position of the element and the scanning angle, the compensation matrix for the pattern function and the array weighted vector with amplitude phase and position errors are derived. At last, the conversion relationship between the array with errors and the array weight vector is corrected in the iterative process. The theoretical simulation experiments verify the effectiveness and robustness of the proposed method for the linear array and rectangular array pattern synthesis. Then, the influence of Taylor expansion order on the pattern synthesis results is analysed.

1. Introduction

Array antennas have been widely utilized in radar, communication, navigation, remote sensing, telemetering, and other fields due to their unique characteristics, such as multifunction, flexible beam control, and high tracking capability [1–3]. In recent years, several excellent and innovative ideas have been proposed for the real application of array antennas. The configurations of the metamaterial photonic bandgap (MTM-PBG) periodic structure and reflector-slot-strip-foam-inverted patch (RSSIP) are used to improve the performance of the densely packed array antenna in synthetic aperture radar (SAR) and multiple-input-multiple-receive (MIMO) systems [4–6]. A novel planar microstrip array antenna is presented based on a simplified composite right/left-handed transmission line (SCRLH-TL) for application in circularly polarized SAR systems in [7]. Meanwhile, a new wideband microstrip antenna based on the falcate-shaped patch is fabricated with the reconfigurable capability of circular polarization [8]. These advanced methods have effectively improved the applicability of the array antennas.

In the application in different fields of the array antennas, several shapes of the array pattern are required which can be formed with different array weights [9–11]. By optimizing the weighted excitation of array elements, a technology that meets the expected demand is formed, which is called array pattern synthesis technology or beamforming technology. In actual engineering applications, different requirements require the array patterns with different shapes. For airborne/spaceborne early warning radar, the observed moving target is in the clutter background, which is widely distributed and with discrete strong clutter [12]. In order to reduce the influence of sidelobe clutter and improve the detection performance of moving targets, the ultralow sidelobe can be formed by the array synthesis technology. Not only like this, it is also necessary to form deep nulls in certain angular ranges to suppress strong clutter points or interference signals in many applications.

To address this issue, several synthesis methods have been proposed in recent years. The array pattern synthesis methods can be classified into three categories: analytical methods [13–15], intelligent algorithms [16–21], and convex optimization methods [22–28]. The analytical synthesis methods such as Chebyshev method, Taylor method, and Woodward-Lawson method are simple to be implemented. The methods can also achieve the smallest peak gain loss and main lobe broadening under certain constraints. However, the Chebyshev synthesis and Taylor synthesis techniques are only suitable for low sidelobe level and cannot form the expected pattern of other shapes. The Woodward-Lawson synthesis is a classic and effective synthesis method. But the synthesis results are with high sidelobe using the sinc function. The intelligent optimization methods including genetic algorithms and simulated annealing can realize the synthesis of the pattern of various shapes by associating the cost function with the shape of the pattern and constraining the magnitude and phase of the weight vector in the iterative process. However, intelligent optimization methods often require multidimensional parameter optimization, and the calculation complexity of the intelligent optimization method increases rapidly as the array size becomes larger. Meanwhile, the local convergence is more likely to produce. The convex optimization methods are also a type of method to solve the pattern synthesis by converting the pattern synthesis problem into a constraint problem. These methods can easily constrain the performance of the pattern, but they also face the problem of huge amount of calculation for the synthesis of large aperture arrays.

In recent years, the iterative fast Fourier transform (FFT) synthesis method has been proposed for uniformly distributed large aperture arrays by Keizer et al. creatively [29–31]. The advantages of this method, which is especially suitable for pattern synthesis of large aperture arrays, are that they can complete the pattern synthesis fast, efficiently, and with strong convergence. The important prerequisite for the application of this method is the property that the array elements are periodically spaced and without array errors. However, due to the influence of factors such as antenna assembly and integration, thermal load, and aging of the array elements, the amplitude-phase errors and position errors of each element of the large aperture array are unavoidable. Then, the property for array elements with periodic spacing can be destroyed by array errors, and the performance may be decreased in practical application.

This paper considers the large aperture array synthesis method in the presence of amplitude-phase errors and position errors. The amplitude-phase response errors and position errors of each element can be obtained in real time by the internal calibration and the external calibration [32, 33]. Based on this, for large aperture arrays in the presence of array errors, an improved iterative discrete Fourier transform (DFT) synthesis method is proposed, in which the influence of array errors is compensated. The Taylor expansion method is used to remove the coupling relationship between the position of the array element and the scanning angle. Thereby, the pattern function and the array weighted compensation matrix are derived in the presence of amplitude-phase and position errors. After the iterations, the accurate pattern synthesis results can be obtained. Simulation experiments verify the effectiveness and robustness of the algorithm for the synthesis of large aperture for linear array and two-dimensional array.

2. Fast Array Pattern Synthesis Approach

We assume an ideal n-element linear array with half-wavelength spacing, and $\mathbf{w} = [w_0, w_1, \ldots, w_{N-1}]^T$ is the array excitation vector. The position vectors in X-axis and Y-axis are denoted by $\mathbf{x}_0 = [x_0^0, x_1^0, \ldots x_{N-1}^0]^T$ and $\mathbf{y}_0 = [y_0^0, y_1^0, \ldots y_{N-1}^0]^T$, where $x_n^0 = \mathrm{nd}$ and $y_n^0 = 0$ are the nominal coordinates of the nth element in X-axis and Y-axis, respectively, $\mathrm{d} = \lambda/2$ is the element spacing of the linear array, and λ is the wavelength.

The array pattern can be obtained by multiplying the array factor and the array element pattern. The array pattern that only needs to consider the array factor is given by

$$\mathbf{f}_0(u) = \sum_{n=0}^{N-1} w_0(n) e^{j(2\pi/\lambda)x_n^0 u} = \sum_{n=0}^{N-1} \mathbf{w}_0(n) e^{j(2\pi/\lambda)n\mathrm{d}u}, \quad (1)$$

where u is the uniform sampling in $[-1, 1]$, $u = \cos\theta$ and $u \in [-1, 1]$. Obviously, DFT and inverse discrete Fourier transform (IDFT) can be used to transform between the pattern function $\mathbf{f}$ of the uniform linear array and the excitation weight vector $\mathbf{w}$ of the array element as follows:

$$\begin{aligned} \mathbf{f} &\longrightarrow \mathrm{IDFT}[\mathbf{w}], \\ \mathbf{w} &\longleftarrow \mathrm{DFT}[\mathbf{f}], \end{aligned} \quad (2)$$

where $\mathrm{DFT}[\cdot]$ is the DFT operation and $\mathrm{IDFT}[\cdot]$ is the IDFT operation.

For the large rectangular arrays, literature [29] introduces the fast Fourier techniques (FFTs) into the pattern synthesis technique. This method utilizes the Fourier transform relationship between the pattern function of the periodic array and the excitation vector of the array. Then, the pattern and weighting vector are corrected iteratively according to the expected sidelobe level. Because this method is based on DFT calculation, it has the advantages of being fast and efficient. However, this method may fail with the unavoidable array errors.

3. Proposed Array Synthesis Methods

We assume that the real array element position vectors are $\mathbf{x} = [x_0, x_1, \ldots, x_{N-1}]^T$ and $\mathbf{y} = [y_0, y_1, \ldots y_{N-1}]^T$, which can be given by

$$\begin{aligned} x_n &= x_n^0 + \Delta x_n, \\ y_n &= \Delta y_n, \end{aligned} \quad (3)$$

where $\Delta\mathbf{x} = [\Delta x_0, \ldots, \Delta x_{N-1}]^T$ and $\Delta\mathbf{y} = [\Delta y_0, \ldots, \Delta y_{N-1}]^T$ are the array position error vectors and Δx_n and Δy_n are the position error of the corresponding array element on X-axis and Y-axis.

The actual pattern with the amplitude-phase errors and position errors can be formulated as

$$\begin{aligned}\mathbf{f}(u) &= \sum_{n=0}^{N-1} \mathbf{w}(n)\Gamma(n)e^{j(2\pi/\lambda)\left(x_n u + y_n v\right)}, \\ &= \sum_{n=0}^{N-1} \mathbf{w}(n)\Gamma(n)e^{j(2\pi/\lambda)\left\{\left(x_n^0 + \Delta x_n\right)u + \Delta y_n v\right\}},\end{aligned} \tag{4}$$

where $v = \sqrt{1-u^2} = \sin\theta$, $\Gamma = [\Gamma(0), \ldots, \Gamma(N-1)]^T$, and $\Gamma(n)$ is the amplitude-phase error of the nth element.

The amplitude-phase deviation caused by amplitude-phase errors has no dependence on the angle, while the phase error caused by the position error is different in different scanning angles. Consider using the Taylor expansion method to eliminate the coupling of position error and scanning angle in phase error. The K-order Taylor expansion of the error term which is introduced by the position errors is obtained as follows:

$$\begin{aligned}e^{j(2\pi/\lambda)\left(\Delta x_n u + \Delta y_n^v\right)} &\cong 1 + \mathbf{d}(n,u) + \frac{1}{2!}\mathbf{d}^2(n,u) \\ &\quad + \cdots + \frac{1}{K!}\mathbf{d}^K(n,u),\end{aligned} \tag{5}$$

where $\mathbf{d}(n,u) = \mathbf{d}_x(n)u + \mathbf{d}_y(n)v$, $\mathbf{d}_x(n) = j(2\pi/\lambda)\Delta\mathbf{x}_n$, and $\mathbf{d}_y(n) = j2\pi/\lambda\Delta\mathbf{y}_n$. And, it is required that the array error disturbance $|\Delta x_n u + \Delta y_n v|$ cannot be greater than the wavelength, which is satisfied in almost all scenes.

Based on (4) and (5), we have

$$\begin{aligned}\mathbf{f}(u) &\cong \sum_{n=0}^{N-1} \mathbf{w}(n)\Gamma(n)e^{j(2\pi/\lambda)x_n^0 u} + \sum_{n=0}^{N-1} \mathbf{w}(n)\Gamma(n)\mathbf{d}(n,u)e^{j(2\pi/\lambda)x_n^0 u} \\ &\quad + \cdots + \frac{1}{K!}\sum_{n=0}^{N-1} \mathbf{w}(n)\Gamma(n)\mathbf{d}^K(n,u)e^{j(2\pi/\lambda)x_n^0 u} = \sum_{k=0}^{K}\sum_{n=0}^{N-1} \frac{1}{k!}\mathbf{w}(n)\Gamma(n)\mathbf{d}^k(n,u)e^{j(2\pi/\lambda)x_n^0 u},\end{aligned} \tag{6}$$

where the polynomial expansion of $\mathbf{d}^k(n,u)$ is

$$\mathbf{d}^k(n,u) = \sum_{q=0}^{k} C_k^q \mathbf{d}_x^q(n)\mathbf{d}_y^{k-q}u^q v^{k-q}, \tag{7}$$

where $C_k^q = k!/q!(k-q)!$. Based on (6) and (7), we have

$$\begin{aligned}\mathbf{f}(u) &\cong \sum_{k=0}^{K}\sum_{n=0}^{N-1} \frac{1}{K!}\mathbf{w}(n)\Gamma(n)\mathbf{d}^k(n,u)e^{j(2\pi/\lambda)x_n^0 u}, \\ &= \sum_{k=0}^{K}\sum_{q=0}^{K}\sum_{n=0}^{N-1} \frac{C_k^q}{K!}\mathbf{w}(n)\Gamma(n)\mathbf{d}_x^q(n)\mathbf{d}_y^{k-q}(n)u^q v^{k-q}e^{j(2\pi/\lambda)x_n^0 u}.\end{aligned} \tag{8}$$

Therefore, using Taylor expansion and the time-domain circular convolution, the pattern function is expressed in the form of multiple DFTs:

$$\begin{aligned}\mathbf{f} &= \sum_{k=0}^{K}\sum_{q=0}^{K} \frac{C_k^q}{k!}u^q \odot v^{k-q} \odot \mathrm{IDFT}\left[\mathbf{d}_x^q \odot \mathbf{d}_y^{k-q} \odot \Gamma \odot \mathbf{w}\right], \\ &= \sum_{k=0}^{K}\sum_{q=0}^{K} \frac{C_k^q}{k!}u^q \odot v^{k-q} \odot \left(\mathrm{IDFT}\left[\mathbf{d}_x^q \odot \mathbf{d}_y^{k-q} \odot \Gamma\right] * \mathrm{IDFT}[\mathbf{w}]\right), \\ &= \sum_{k=0}^{K}\sum_{q=0}^{K} \frac{C_k^q}{k!}\mathrm{diag}\left(u^q \odot v^{k-q}\right)\mathbf{C}_1\mathrm{IDFT}\left[\mathbf{d}_x^q \odot \mathbf{d}_y^{k-q} \odot \Gamma\right]\mathrm{IDFT}[\mathbf{w}], \\ &= \mathrm{TIDFT}[\mathbf{w}],\end{aligned} \tag{9}$$

where $\odot$ denotes the dot product operation, $*$ denotes the circular convolution operation, and $\mathbf{T}$ is the compensation matrix of Fourier transform as follows:

$$\mathbf{T} = \sum_{k=0}^{K}\sum_{q=0}^{k} \frac{C_k^q}{k!}\mathrm{diag}\left(u^q \odot v^{k-q}\right)C_1\mathrm{IDFT}\left[\mathbf{d}_x^q \odot \mathbf{d}_y^{k-q} \odot \Gamma\right], \tag{10}$$

where $\mathbf{C}_1\cdot$ denotes the calculation of a cyclic convolution matrix operation. For any vector $\mathbf{b}$ of length M, the cyclic convolution matrix of $\mathbf{b}$ is given by

$$\mathbf{C}_1\mathbf{b} = \begin{bmatrix} \mathbf{b}(1) & \mathbf{b}(M) & \mathbf{b}(M-1) & \cdots & \mathbf{b}(2) \\ \mathbf{b}(2) & \mathbf{b}(1) & \mathbf{b}(M) & \cdots & \mathbf{b}(3) \\ \mathbf{b}(3) & \mathbf{b}(0) & \mathbf{b}(1) & \cdots & \mathbf{b}(4) \\ \vdots & \vdots & \vdots & \ddots & \vdots \\ \mathbf{b}(M) & \mathbf{b}(M-1) & \mathbf{b}(M-2) & \cdots & \mathbf{b}(1) \end{bmatrix}. \tag{11}$$

According to (9), the weighted vector of the array is given as follows:

$$\mathbf{w} = \mathrm{DFT}\left[\mathbf{T}^{-1}\mathbf{f}\right]. \tag{12}$$

There, the specific iterative steps of the proposed improved method are given as follows:

(1) Set expected pattern parameters, Taylor expansion order, and threshold of two adjacent excitation errors ε_0. If the purpose of the pattern synthesis is only to control the sidelobe level, the pattern parameters include the left and right sidelobe levels.

(2) According to the given array parameters, the Fourier transform compensation matrix $\mathbf{T}$ and its inverse matrix $\mathbf{T}^{-1}$ can be calculated using formula (10).

(3) Initialize the array excitation vector $\mathbf{w}$, and set the number of iterations $l = 0$.

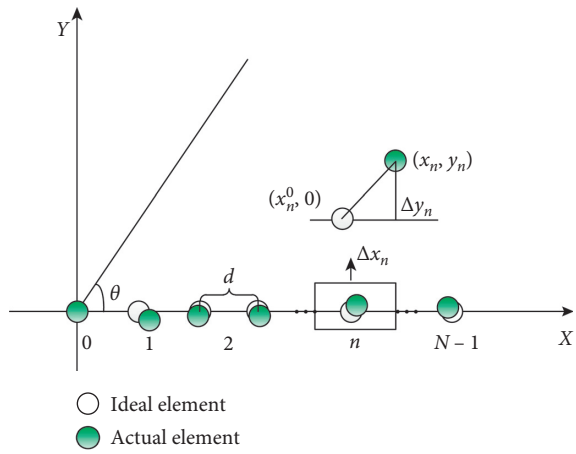

Figure 1: Configuration of the linear array with position errors.

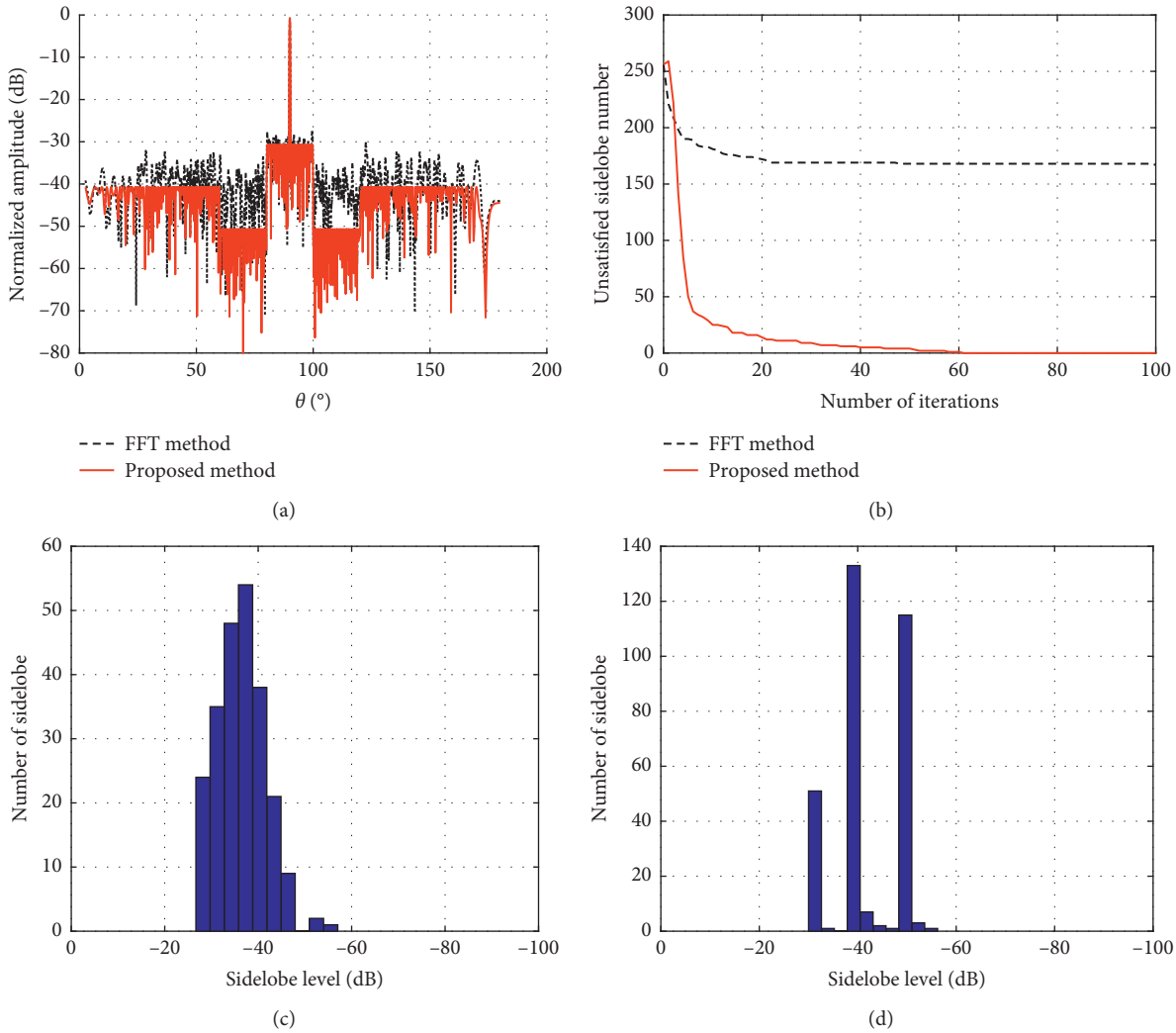

Figure 2: Linear array synthesis results. (a) Pattern results of the two method. (b) Number of the sidelobe that unsatisfied the requirements versus the iteration number. (c) The sidelobe level distribution histogram of the conventional method. (d) The sidelobe level distribution histogram of the proposed method.

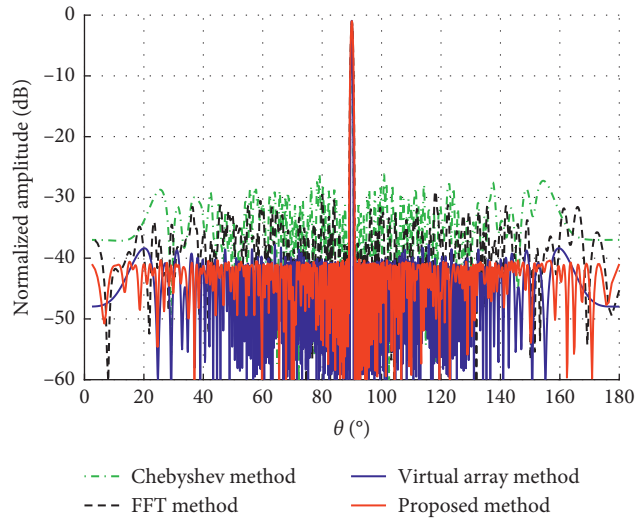

Figure 3: The pattern synthesis results of several methods.

Table 1: The sidelobe level count of the pattern synthesis methods in the simulation.

Method	Sidelobe number	Sidelobe number (SLL < −40 dB)	Ratio (%)
Chebyshev method	113	5	4.42
FFT method	118	22	18.64
Virtual array method	198	166	83.83
Proposed method	162	161	99.38

(4) Perform IDFT operation on the array weight vector, and perform error compensation on the obtained directional pattern function $\mathbf{f}^l$ according to formula (9).

(5) According to the expected pattern parameters, correct the pattern function and update $\mathbf{f}^l$.

(6) Perform DFT operation on the updated pattern function, and use equation (12) to perform error compensation on the weighted vector obtained. Take the first n elements as the weight vector and normalize it after this iteration.

(7) Calculate the root mean square error (RMS) of two adjacent weight vectors $\varepsilon^l = \sqrt{1/N \sum_{n=0}^{N-1} (\mathbf{w}^l(n) - \mathbf{w}^{l-1}(n))^2}$. Judge whether the convergence condition is satisfied. If $\varepsilon^l > \varepsilon_0$, then let $l = l + 1$ and skip to step 4. Otherwise, terminate the iteration and output the array excitation $\mathbf{w}^l$.

4. Simulation Results

In this section, the simulations are performed for the pattern synthesis of the linear array and the planar array. The working wavelength of the arrays is 0.2308 m. The actual arrays are with the amplitude-phase errors and the position errors. Array errors are independent and identically distributed random variables. In the following simulations, the amplitude-phase error RMS is 0.1 dB/0.1° and the position error RMS is denoted by $d_{\max}$. Meanwhile, the measurement accuracy of the array deformation calibration equipment or method is millimeter level.

4.1. Synthesis of a Linear Array. The uniform linear array is distributed on the X-Y plane, as shown in Figure 1, of which the number of array elements is 400. Figure 2 shows the synthesis result of the linear array pattern using the conventional DFT method and the proposed synthesis method in this paper. The position error RMS $d_{\max}$ is 0.05λ. The number of DFT points is 2048, and the Taylor expansion order K of the proposed method is 3.

The sidelobe requirements are −40 dB in the 0°–60° interval, −50 dB in the 60°–80° interval, −30 dB in the 80°–100° interval, −50 dB in the interval of 100°–120°, and −40 dB in the interval of 120°–180°, and the sidelobe of the pattern is symmetrical about 90°. The number of sidelobes that do not satisfy the sidelobe constraints versus the iteration number is shown in Figure 2(b). Figures 2(c) and 2(d) show the histogram of the sidelobe level distribution of the two methods, respectively. It can be found that the classical iterative DFT method has obvious elevation of the sidelobes for the array with the position error of the array elements and the improved method can obtain the accurate synthesis result of the pattern efficiently and quickly.

Next, the linear array is applied to compare the proposed method with the Chebyshev method, FFT method, and virtual array method. Suppose that the number of linear array elements is 400, the sidelobe requirement is −40 dB, and the position error RMS $d_{\max}$ is 0.1 λ. Figure 3 and Table 1 show the pattern synthesis results of the four methods. It can be found that the sidelobe levels (SLL) in the proposed method are basically below −40 dB with the ratio of 99.38%.

Figures 4 and 5 show the pattern synthesis and sidelobe level distribution histogram results versus K. It can be found

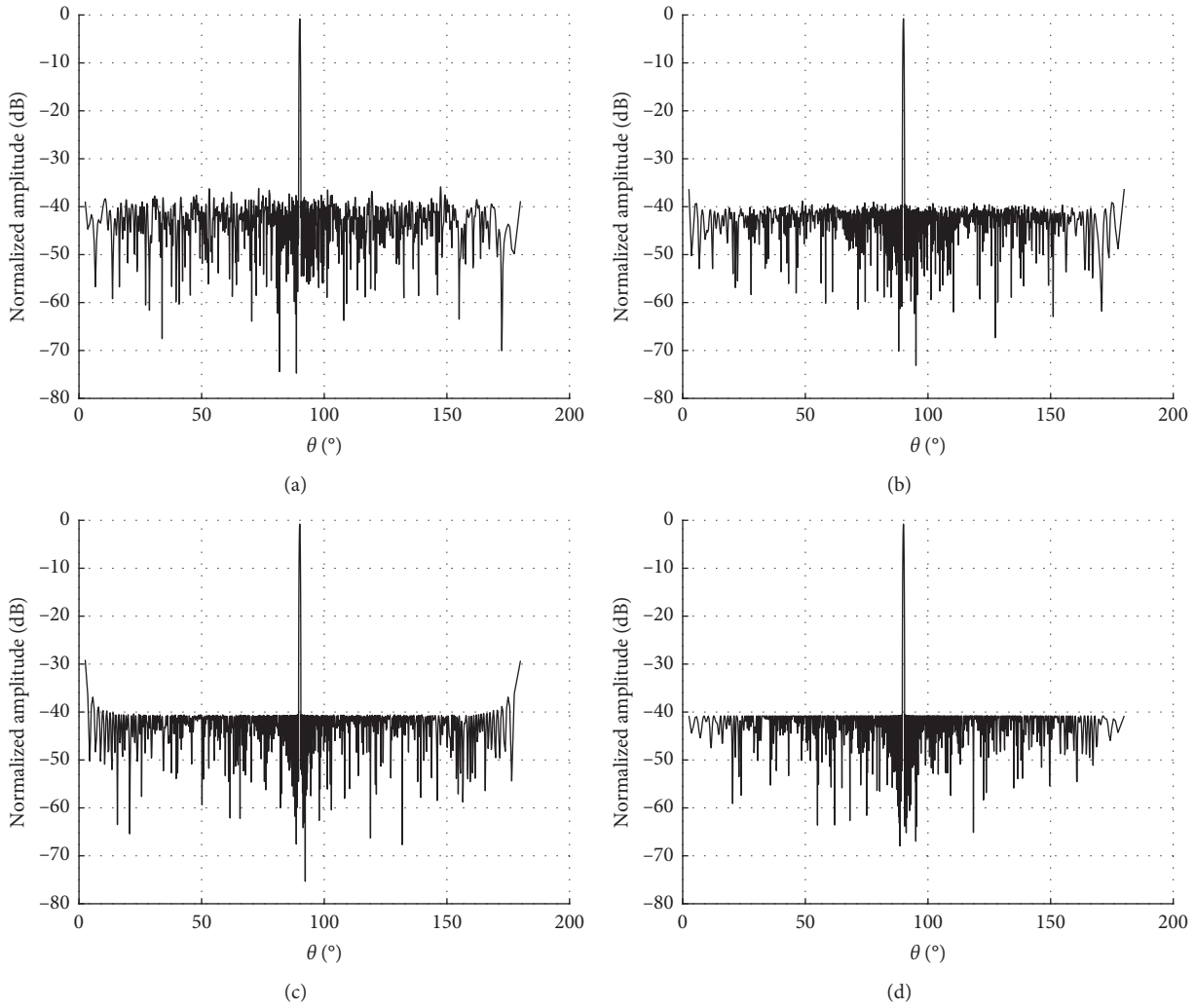

Figure 4: The pattern synthesis results of the proposed method versus the Taylor expansion order. (a) $K = 1$. (b) $K = 2$. (c) $K = 3$. (d) $K = 4$.

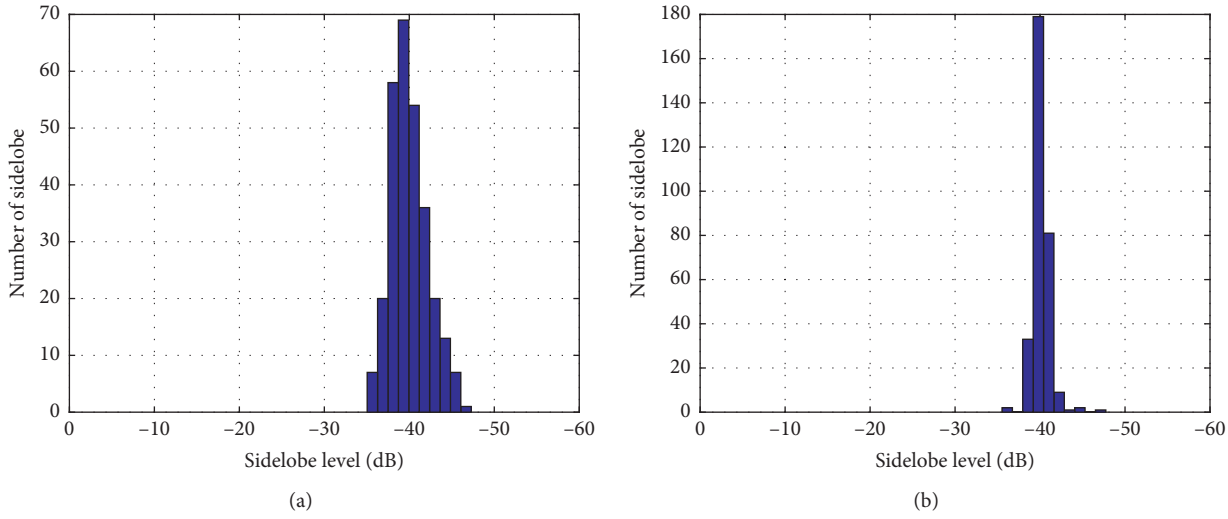

Figure 5: Continued.

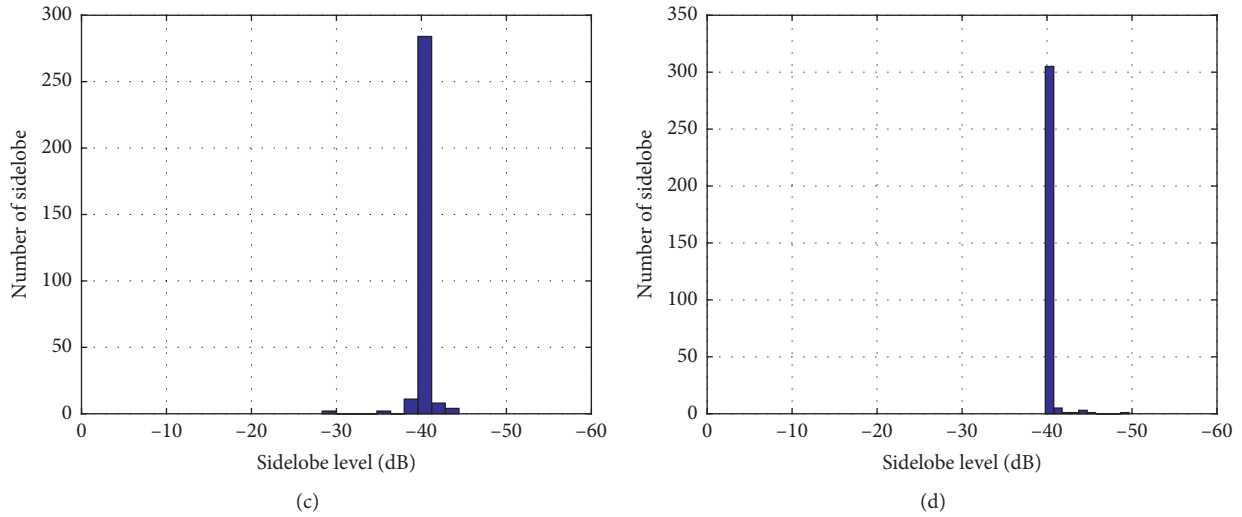

FIGURE 5: The sidelobe level distribution histogram of the proposed method versus the Taylor expansion order. (a) $K = 1$. (b) $K = 2$. (c) $K = 3$. (d) $K = 4$.

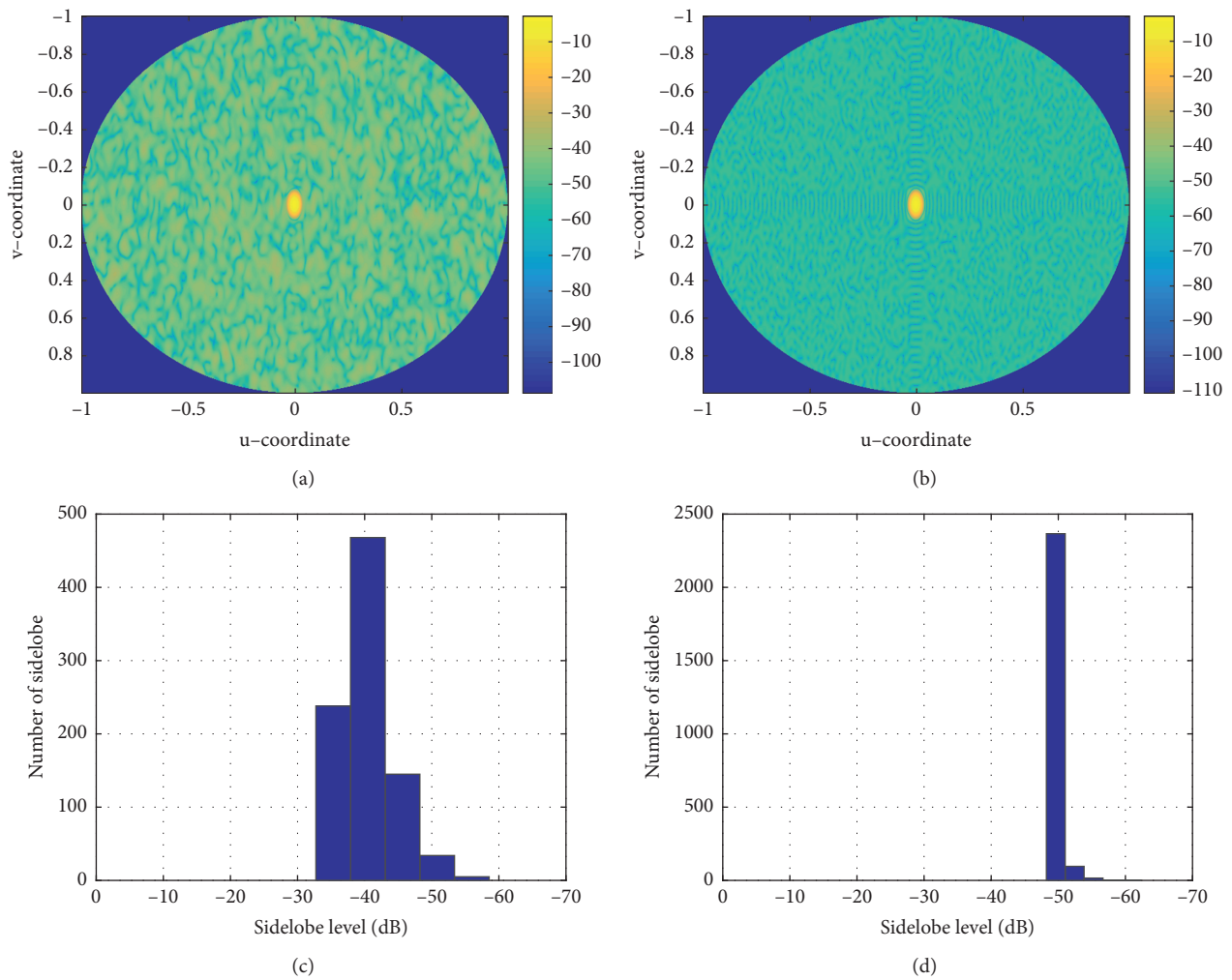

FIGURE 6: Rectangular array synthesis results. (a) Synthesis results of the conventional method. (b) Synthesis results of the improved method. (c) Sidelobe histogram of the conventional method. (d) Sidelobe histogram of the improved method.

that, with the increase of the Taylor expansion order, the distribution of sidelobe levels gradually concentrates below the sidelobe level required. When the order K is 3 or 4, the synthesis result can probably meet the requirements under this simulation conditions.

4.2. Synthesis of a Planar Array. The rectangular array consists of 5000 elements. The row number is 50, and the column number is 100. The synthesis results of the array pattern using the classical DFT method and the error compensation DFT method in this paper are shown in Figure 6. The sidelobe level required is −50 dB, and the three-dimensional position error RMS $d_{\max}$ is 0.05λ. The Taylor expansion order of the method in this section in Figures 6(b) and 6(d) is 5. There are high-level sidelobes in the results of the conventional synthesis method. It can be noted that the improved method can still obtain better results than the conventional method for two-dimensional arrays.

5. Conclusion

This paper has described an improved pattern synthesis method for the large aperture array in the presence of array errors. The compensation for the amplitude-phase errors and positions errors is derived to correct the relationship between the array pattern and weighted vector. Compared with the conventional method, the improved method is more effective and robust for the large array with amplitude-phase and position errors. At the same time, the pattern synthesis of multiple sidelobes and the influence of Taylor expansion order on the results are simulated, which provides guidance for the parameter selection in subsequent actual projects.

Data Availability

The data used to support the findings of this study are available from the corresponding author upon request.

Conflicts of Interest

The authors declare that there are no conflicts of interest regarding the publication of this paper.

Acknowledgments

This study was supported by the Central Government Guides Local Technology Development Funds (206Z0701G).

References

[1] C. Luison, A. Landini, P. Angeletti et al., "Aperiodic arrays for spaceborne SAR applications," *IEEE Transactions on Antennas and Propagation*, vol. 60, no. 5, pp. 2285–2294, 2012.

[2] C. Heer and C. Schaefer, "Digital beam forming technology for phased array antennas," in *Proceedings of the 2011 2nd International Conference on Space Technology*, pp. 1–4, Athens, Greece, September 2011.

[3] N. Chamberlain, L. Amaro, E. Oakes, R. Hodges, S. Spitz, and P. A. Rosen, "Microstrip patch antenna panel for large aperture L-Band phased array," in *Proceedings of the IEEE Aerospace Conference*, pp. 1185–1192, Big Sky, MT, USA, March 2005.

[4] M. Alibakhshikenari, B. S. Virdee, and P. Shukla, "Isolation enhancement of densely packed array antennas with periodic MTM-Photonic bandgap for SAR and MIMO systems," *IET Microwaves Antennas and Propagation*, vol. 14, no. 3, pp. 183–188, 2020.

[5] M. Alibakhshikenari, M. Khalily, B. S. Virdee, C. H. See, R. A. Abd-Alhameed, and E. Limiti, "Mutual-coupling isolation using embedded metamaterial EM bandgap decoupling slab for densely packed array antennas," *IEEE Access*, vol. 7, pp. 51827–51840, 2019.

[6] M. M. Shirkolaei, "High efficiency X-band series-fed microstrip array antenna," *Progress In Electromagnetics Research C*, vol. 105, pp. 35–45, 2020.

[7] M. Alibakhshikenari, B. S. Virdee, and E. Limiti, "Wideband planar array antenna based on SCRLH-TL for airborne synthetic aperture radar application," *Journal of Electromagnetic Waves and Applications*, vol. 32, no. 12, pp. 1586–1599, 2020.

[8] M. M. Shirkolaei and M. Jafari, "A new class of wideband microstrip falcate patch antennas with reconfigurable capability at circular-polarization," *Microwave and Optical Technology Letters*, vol. 62, no. 12, pp. 1–6, 2020.

[9] S. Hema and J. R. Mohan, "Trends in adaptive array processing," *International Journal of Antennas and Propagation*, vol. 2012, Article ID 361768, 20 pages, 2012.

[10] W. Croswell, "Antenna theory, analysis, and design," *IEEE Antennas and Propagation Society Newsletter*, vol. 24, no. 6, pp. 28-29, 1982.

[11] M. M. Shirkolaei, "Wideband linear microstrip array antenna with high efficiency and low side lobe level," *International Journal of RF and Microwave Computer-Aided Engineering*, vol. 30, no. 1, 2020.

[12] W. L. Melvin, "A STAP overview," *IEEE Aerospace and Electronic Systems Magazine*, vol. 19, no. 1, pp. 19–35, 2004.

[13] R. Elliott, "Design of line source antennas for narrow beamwidth and asymmetric low sidelobes," *IEEE Transactions on Antennas and Propagation*, vol. 23, no. 1, pp. 100–107, 1975.

[14] K. Yang, Z. Zhao, and Q. H. Liu, "Fast pencil beam pattern synthesis of large unequally spaced antenna arrays," *IEEE Transactions on Antennas and Propagation*, vol. 61, no. 2, pp. 627–634, 2013.

[15] A. E. Taser, K. Guney, and E. Kurt, "Circular antenna array synthesis using multiverse optimizer," *International Journal of Antennas and Propagation*, vol. 2020, Article ID 3149826, 10 pages, 2016.

[16] E. Rajo-Iglesias and O. Quevedo-Teruel, "Linear array synthesis using an ant-colony-optimization-based algorithm," *IEEE Antennas and Propagation Magazine*, vol. 49, no. 2, pp. 70–79, 2007.

[17] R. Bhattacharya, T. K. Bhattacharyya, and R. Garg, "Array pattern synthesis using particle swarm optimization with dynamic inertia weight," *International Journal of Antennas and Propagation*, vol. 2016, p. 7, Article ID 1829458, 2016.

[18] R. Bhattacharya, T. K. Bhattacharyya, and R. Garg, "Position mutated hierarchical particle swarm optimization and its application in synthesis of unequally spaced antenna arrays," *IEEE Transactions on Antennas and Propagation*, vol. 60, no. 7, pp. 3174–3181, 2012.

[19] L. Shi, Y.-k. Deng, H.-f. Sun, R. Wang, J.-q. Ai, and H. Yan, "An improved real-coded genetic algorithm for the beam

forming of spaceborne SAR," *IEEE Transactions on Antennas and Propagation*, vol. 60, no. 6, pp. 3034–3040, 2012.

[20] G. He, Y. Zhan, Y. Pei, and B. Wu, "Subarrayed antenna array synthesis using ternary adjusting method," *International Journal of Antennas and Propagation*, vol. 2014, Article ID 898717, 5 pages, 2014.

[21] C. Han and L. Wang, "Array pattern synthesis using particle swarm optimization with dynamic inertia weight," *International Journal of Antennas and Propagation*, vol. 2016, Article ID 1829458, 7 pages, 2016.

[22] Z. Chen, T. Li, and D. Peng, "Two-dimensional beampattern synthesis for polarized smart antenna array and its sparse array optimization," *International Journal of Antennas and Propagation*, vol. 2020, Article ID 2196049, 13 pages, 2020.

[23] H. Lebret and S. Boyd, "Antenna array pattern synthesis via convex optimization," *IEEE Transactions on Signal Processing*, vol. 45, no. 3, pp. 526–532, 1997.

[24] S. Lei, Y. Yang, H. Hu, Z. Zhao, B. Chen, and X. Qiu, "Power gain optimization method for wide-beam array antenna via convex optimization," *IEEE Transactions on Antennas and Propagation*, vol. 67, no. 3, pp. 1620–1629, 2019.

[25] N. Anselmi, P. Rocca, M. Salucci, and A. Massa, "Optimisation of excitation tolerances for robust beamforming in linear arrays," *IET Microwaves, Antennas & Propagation*, vol. 10, no. 2, pp. 208–214, 2016.

[26] P. Rocca, N. Anselmi, and A. Massa, "Optimal synthesis of robust beamformer weights exploiting interval analysis and convex optimization," *IEEE Transactions on Antennas and Propagation*, vol. 62, no. 7, pp. 3603–3612, 2014.

[27] K. Guney, A. Durmus, and S. Basbug, "Antenna array synthesis and failure correction using differential search algorithm," *International Journal of Antennas and Propagation*, vol. 2014, Article ID 276754, 8 pages, 2014.

[28] L. Liang, Y. Jiang, J. Liu, H. Li, and J. Zhou, "Pattern synthesis of time-modulated sparse array by an OPM-CVX algorithm," *Mathematical Problems in Engineering*, vol. 2020, Article ID 5491921, 15 pages, 2020.

[29] W. P. M. N. Keizer, "Fast low-sidelobe synthesis for large planar array antennas utilizing successive fast fourier transforms of the array factor," *IEEE Transactions on Antennas and Propagation*, vol. 55, no. 3, pp. 715–722, 2007.

[30] W. P. M. N. Keizer, "Amplitude-only low sidelobe synthesis for large thinned circular array antennas," *IEEE Transactions on Antennas and Propagation*, vol. 60, no. 2, pp. 1157–1161, 2012.

[31] W. P. M. N. Keizer, "APAS: an advanced phased-array simulator," *IEEE Antennas and Propagation Magazine*, vol. 52, no. 2, pp. 40–56, 2010.

[32] D. McWatters, A. Freedman, T. Michel, and V. Cable, "Antenna auto-calibration and metrology approach for the AFRL/JPL space based radar," in *Proceedings of the 2004 IEEE Radar Conference*, pp. 21–26, Philadelphia, PA, USA, July 2004.

[33] J. Guerci and E. Jaska, "ISAT-innovative space-based-radar antenna technology," in *Proceedings of the IEEE International Symposium on Phased Array Systems and Technology*, pp. 45–51, Boston, MA, USA, October 2003.